

NEA Nuclear Science Committee
NEA Committee on Safety of Nuclear Installations
US Nuclear Regulatory Commission

NUPEC BWR Full-size Fine-mesh Bundle Test (BFBT) Benchmark

***Volume II: Uncertainty and Sensitivity Analyses of
Void Distribution and Critical Power – Specification***

F. Aydogan, L. Hochreiter, K. Ivanov
The Pennsylvania State University

M. Martin
Commissariat à l'Énergie Atomique

H. Utsuno
Japan Nuclear Energy Safety Organization

E. Sartori
OECD Nuclear Energy Agency

© OECD 2010
NEA No. 6343

NUCLEAR ENERGY AGENCY
Organisation for Economic Co-operation and Development

ORGANISATION FOR ECONOMIC CO-OPERATION AND DEVELOPMENT

The OECD is a unique forum where the governments of 31 democracies work together to address the economic, social and environmental challenges of globalisation. The OECD is also at the forefront of efforts to understand and to help governments respond to new developments and concerns, such as corporate governance, the information economy and the challenges of an ageing population. The Organisation provides a setting where governments can compare policy experiences, seek answers to common problems, identify good practice and work to co-ordinate domestic and international policies.

The OECD member countries are: Australia, Austria, Belgium, Canada, Chile, the Czech Republic, Denmark, Finland, France, Germany, Greece, Hungary, Iceland, Ireland, Italy, Japan, Korea, Luxembourg, Mexico, the Netherlands, New Zealand, Norway, Poland, Portugal, the Slovak Republic, Spain, Sweden, Switzerland, Turkey, the United Kingdom and the United States. The Commission of the European Communities takes part in the work of the OECD.

OECD Publishing disseminates widely the results of the Organisation's statistics gathering and research on economic, social and environmental issues, as well as the conventions, guidelines and standards agreed by its members.

This work is published on the responsibility of the Secretary-General of the OECD. The opinions expressed and arguments employed herein do not necessarily reflect the official views of the Organisation or of the governments of its member countries.

NUCLEAR ENERGY AGENCY

The OECD Nuclear Energy Agency (NEA) was established on 1st February 1958 under the name of the OEEC European Nuclear Energy Agency. It received its present designation on 20th April 1972, when Japan became its first non-European full member. NEA membership today consists of 28 OECD member countries: Australia, Austria, Belgium, Canada, the Czech Republic, Denmark, Finland, France, Germany, Greece, Hungary, Iceland, Ireland, Italy, Japan, Luxembourg, Mexico, the Netherlands, Norway, Portugal, Republic of Korea, the Slovak Republic, Spain, Sweden, Switzerland, Turkey, the United Kingdom and the United States. The Commission of the European Communities also takes part in the work of the Agency.

The mission of the NEA is:

- to assist its member countries in maintaining and further developing, through international co-operation, the scientific, technological and legal bases required for a safe, environmentally friendly and economical use of nuclear energy for peaceful purposes, as well as
- to provide authoritative assessments and to forge common understandings on key issues, as input to government decisions on nuclear energy policy and to broader OECD policy analyses in areas such as energy and sustainable development.

Specific areas of competence of the NEA include safety and regulation of nuclear activities, radioactive waste management, radiological protection, nuclear science, economic and technical analyses of the nuclear fuel cycle, nuclear law and liability, and public information.

The NEA Data Bank provides nuclear data and computer program services for participating countries. In these and related tasks, the NEA works in close collaboration with the International Atomic Energy Agency in Vienna, with which it has a Co-operation Agreement, as well as with other international organisations in the nuclear field.

Corrigenda to OECD publications may be found on line at: www.oecd.org/publishing/corrigenda.

© OECD 2010

You can copy, download or print OECD content for your own use, and you can include excerpts from OECD publications, databases and multimedia products in your own documents, presentations, blogs, websites and teaching materials, provided that suitable acknowledgment of OECD as source and copyright owner is given. All requests for public or commercial use and translation rights should be submitted to rights@oecd.org. Requests for permission to photocopy portions of this material for public or commercial use shall be addressed directly to the Copyright Clearance Center (CCC) at info@copyright.com or the Centre français d'exploitation du droit de copie (CFC) contact@cfcopies.com.

Foreword

The need to refine models for best-estimate calculations based on good-quality experimental data has been expressed in many recent meetings concerning nuclear applications. The needs arising in this respect should not be limited to the currently available macroscopic methods but should be extended to next-generation analysis techniques that focus on more microscopic processes. A very valuable database for thermal-hydraulics modelling was developed by the Nuclear Power Engineering Corporation (NUPEC), Japan; it includes sub-channel void fraction measurements in a representative BWR fuel assembly (NEA, 2006). Part of this database has been made available for this international benchmark activity entitled “NUPEC BWR full-size fine-mesh bundle tests (BFBT) benchmark”. This international project has been officially approved by the Japanese Ministry of Economy, Trade and Industry (METI), the US Nuclear Regulatory Commission (NRC) and endorsed by the OECD/NEA. The benchmark team has been organised based on collaboration between Japan and the United States. A large number of international experts have agreed to participate in this programme.

The fine-mesh high-quality sub-channel void fraction and critical power data encourages advancement in understanding and modelling complex, two-phase flow behaviour in real bundles. Considering that the present theoretical approach is relatively immature, the benchmark specification is designed so that it will systematically assess and compare the participants’ analytical models on the prediction of detailed void distributions and critical powers. The development of truly mechanistic models for critical power prediction is currently under way. These innovative models include processes such as void distributions, droplet deposition and liquid film entrainment. The benchmark problem includes both macroscopic and microscopic measurement data. In this context, the sub-channel grade void fraction data are regarded as the macroscopic data and the digitised computer graphic images are the microscopic data, which provide void distribution within a sub-channel.

The NUPEC BFBT benchmark consists of two phases. Each phase consists of different exercises:

- Phase I – Void distribution benchmark
 - Exercise 1 – Steady-state sub-channel grade benchmark
 - Exercise 2 – Steady-state microscopic grade benchmark
 - Exercise 3 – Transient macroscopic grade benchmark
 - Exercise 4 – Uncertainty analysis of the void distribution benchmark
- Phase II – Critical power benchmark
 - Exercise 0 – Steady-state pressure drop benchmark
 - Exercise 1 – Steady-state critical power benchmark
 - Exercise 2 – Transient critical power benchmark
 - Exercise 3 – Uncertainty analysis of the critical power benchmark

In order to study the basic thermal-hydraulics in a single channel, where the concern regarding the cross-flow effect modelling could be removed, an elemental task has been proposed. It consists of two sub-tasks that are placed in each phase of the benchmark scope as follows: Sub-task 1: Void fraction in the elemental channel benchmark; and Sub-task 2: Critical power in the elemental channel benchmark.

This report provides the specification for the uncertainty exercises of the international OECD/NEA, NRC and NUPEC BFBT benchmark problem including the elemental task. The specification was prepared jointly by Pennsylvania State University (PSU), USA and the Japan Nuclear Energy Safety (JNES) Organisation, in co-operation with the OECD/NEA and the Commissariat à l’énergie atomique (CEA Saclay, France). The work is sponsored by the US NRC, METI-Japan, the OECD/NEA and the Nuclear Engineering Program (NEP) of Pennsylvania State University. This uncertainty specification covers the fourth exercise of Phase I (Exercise-I-4), and the third exercise of Phase II (Exercise II-3) as well as the elemental task.

Acknowledgements

The authors would like to thank Professor Hideki Nariai, President of the JNES, Japan, whose support and encouragement in establishing and carrying out this benchmark are invaluable.

This report is the sum of many efforts: those of the participants, the funding agencies and their staff – the METI, Japan, US NRC and the Organisation of Economic Co-operation and Development (OECD). Special appreciation goes to the report reviewer, Maria Avramova from the Pennsylvania State University. Her comments, corrections and suggestions were very valuable and significantly improved the quality of this report. Further, the authors would like to thank Penn State graduate students Jeffrey Lane, James Spring and Douglas Miller for their contribution to the development of the Phenomena Identification Ranking Tables.

The authors wish to express their sincere appreciation for the outstanding support offered by the JNES personnel in providing the test data and discussing the test characteristics.

The authors would also like to acknowledge the contribution of Daniel Caruge and Eric Royer of CEA Saclay, France in enriching this benchmark activity for the uncertainty analyses.

Particularly noteworthy are the efforts of Farouk Eltawila and James Han from US NRC. With their help funding was secured, enabling this project to proceed. We also thank them for their excellent technical advice and assistance.

Table of contents

Foreword.....	3
Chapter 1 Introduction	7
Chapter 2 Definitions of the UA/SA terms	9
2.1 Accuracy	9
2.2 Probability density function.....	9
2.3 Precision	9
2.4 Uncertainty	10
2.5 Sensitivity analysis	11
2.6 Verification and validation	11
Chapter 3 Selection and characterisation of uncertainty input parameters for BFBT benchmark	13
3.1 Uncertainty input parameters for Exercises I-4 and II-3.....	13
3.2 Description of the elemental task.....	14
Chapter 4 Suggested methods to be used in the uncertainty exercises of BFBT benchmark	17
4.1 Step 1: Accuracy analysis	17
4.2 Step 2: Uncertainty analysis	18
Chapter 5 Selection of the exercise cases from the BFBT database	21
5.1 Selected cases for accuracy analysis of void distribution.....	21
5.2 Selected cases for accuracy analysis of critical power.....	22
5.3 Selected cases for uncertainty analysis of void distribution.....	23
5.4 Selected cases for uncertainty analysis of critical power.....	24
5.5 Selected cases for elemental task	25
Chapter 6 Requested output	27
6.1 Introduction	27
6.2 Requested output for Exercise 4 of Phase I.....	27
6.3 Requested output for Exercise 3 of Phase II.....	28
6.4 Requested output for elemental task	29
Chapter 7 Conclusions	31
References	33
Appendix 1: Uncertainty and sensitivity analysis methods.....	35
Appendix 2: PIRT information	39

List of figures

2.3.1	Precision in measurement of variable x	10
3.1.1	Distortions of test assembly observed with fine-mesh void measurement.....	14
3.2.1	Image to quantify the cross-flow	16
4.1.1	Example of predicted critical power versus measured critical power	17
4.1.2	Example of predicted to measured critical power versus quality	18
6.4.1	Example of relation between equilibrium quality and void fraction	30
6.4.2	Structure of annular-mist flow.....	30

List of tables

3.1.1	Estimated accuracy and PDF of the main process parameters.....	14
3.2.1	Geometry and power shape of the elemental channel	15
4.2.1	Estimated accuracy of void distribution measurements	19
5.1.1	Selected cases for accuracy analysis in Exercise 4 of Phase I	21
5.1.2	Test matrix of selected cases for Exercise 4 of Phase I	22
5.1.3	Test numbers of selected cases for Exercise 4 of Phase I	22
5.2.1	Selected cases for Exercise 3 of Phase II.....	22
5.2.2	Test matrix of selected cases for Exercise 3 of Phase II.....	23
5.2.3	Experimental conditions of selected cases for Exercise 3 of Phase II	23
5.3.1	The bundle types used in the BFBT measurements.....	24
5.3.2	Selected cases for uncertainty analysis of void distribution.....	24
5.4.1	Selected cases for uncertainty analysis of critical power.....	24
5.5.1	Reference test matrix for elemental task.....	25
5.5.2	Reference test numbers for the elemental task.....	25
5.5.3	Boundary conditions for the elemental task.....	25
6.2.1	Calculated void distribution from deterministic input parameters.....	27
6.3.1	Calculated critical power from deterministic input parameters	28
6.3.2	The calculated critical power uncertainty output format	29
A2.1	PIRT-1 for steady-state void distribution	39
A2.2	PIRT-2 for steady-state void distribution	39
A2.3	PIRT-3 for steady-state void distribution	40
A2.4	PIRT-4 for steady-state void distribution	40
A2.5	PIRT-1 for steady-state critical power	41
A2.6	PIRT-2 for steady-state critical power	41
A2.7	PIRT-3 for steady-state critical power	41
A2.8	PIRT-4 for steady-state critical power	42
A2.9	Comparison of two independent expert groups' decisions about the PIRT tables for the void distribution.....	42
A2.10	Comparison of two independent expert groups' decisions about the PIRT tables for the critical power	42

Chapter 1: Introduction

The OECD/NRC BFBT benchmark provides a very good opportunity to apply uncertainty analysis (UA) and sensitivity analysis (SA) techniques and to assess the accuracy of thermal-hydraulic models for two-phase flows in rod bundles. During the previous OECD benchmarks, participants usually carried out sensitivity analysis on their models for the specification (initial conditions, boundary conditions, etc.) to identify the most sensitive models or/and to improve the computed results. The comprehensive BFBT experimental database (NEA, 2006) leads us one step further in investigating modelling capabilities by taking into account the uncertainty analysis in the benchmark. The uncertainties in input data (boundary conditions) and geometry (provided in the benchmark specification) as well as the uncertainties in code models can be accounted for to produce results with calculational uncertainties and compare them with the measurement uncertainties. Therefore, uncertainty analysis exercises were defined for the void distribution and critical power phases of the BFBT benchmark.

This specification is intended to provide definitions related to UA/SA methods, sensitivity/uncertainty parameters, suggested probability distribution functions (PDF) of sensitivity parameters, and selected experimental cases from the BFBT database for both steady-state void distribution and steady-state critical power uncertainty analyses.

In order to study the basic thermal-hydraulics in a single channel, where the concern regarding the cross-flow effect modelling could be removed, an elemental task is proposed, consisting of two sub-tasks that are placed in each phase of the benchmark scope as follows:

- Sub-task 1: Void fraction in elemental channel benchmark
- Sub-task 2: Critical power in elemental channel benchmark

The first task can also be utilised as an uncertainty analysis exercise for fine computational fluid dynamics (CFD) models for which the full bundle sensitivity or uncertainty analysis is more difficult. The task is added to the second volume of the specification as an optional exercise.

Chapter 2 of this document provides the definition of UA/SA terms.

Chapter 3 provides the selection and characterisation of the input uncertain parameters for the BFBT benchmark and the description of the elemental task.

Chapter 4 describes the suggested approach for UA/SA of the BFBT benchmark.

Chapter 5 provides the selection of data sets for the uncertainty analysis and the elemental task from the BFBT database.

Chapter 6 specifies the requested output for void distribution and critical power uncertainty analyses (Exercises I-4 and II-3) as well as for the elemental task.

Chapter 7 provides conclusions.

Appendix 1 discusses the UA/SA methods.

Appendix 2 presents the Phenomena Identification Ranking Tables (PIRT) developed at PSU for void distribution and critical power predictions in order to assist participants in selecting the most sensitive/uncertain code model parameters.

Chapter 2: Definitions of the UA/SA terms

Definitions of commonly used uncertainty analysis terms are given below.

2.1 Accuracy

Accuracy is the closeness of agreement between the measured value and the true value (Wheeler, 1996).

2.2 Probability density function

The $f(x)dx$ is the probability that the random variable (x) will assume a value in the range of x and $x + dx$. Note that $f(x)$ is defined such that the probability of getting some value x in the range $[a,b]$ is equal to 1. This function, $f(x)$ is called *probability density function (PDF)*. The *cumulative distribution function (CDF)* is defined as:

$$F(x) = \int_a^x dx' f(x')$$

The PDF is normalised such that its corresponding CDF varies in a range of $[0,1]$:

$$0 \leq F(x) \leq 1$$

for all values of x and:

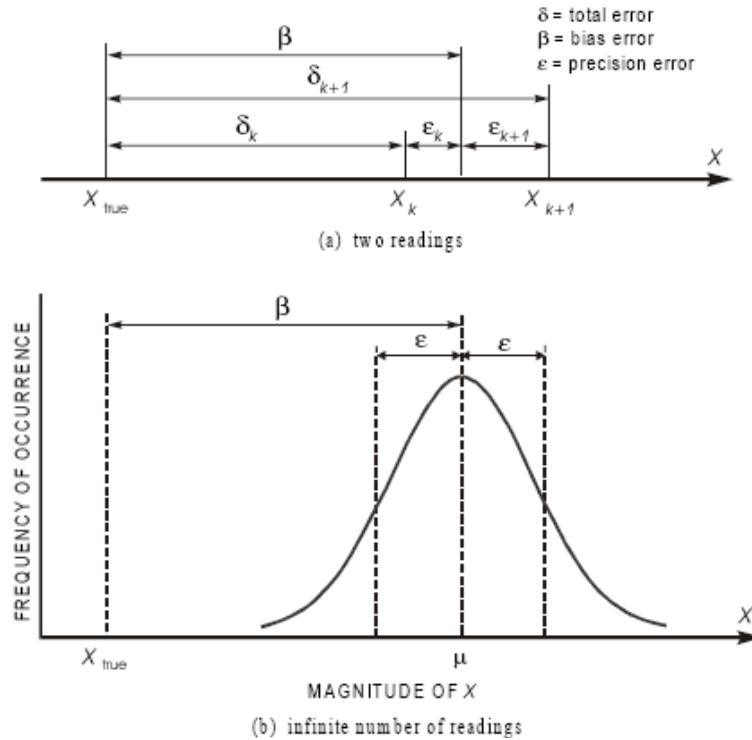
$$F(x) = \int_a^b f(x)dx = 1$$

For the input variable (x) within the range $a \leq x \leq b$, the following classical probability density functions $f(x)$ can be defined:

PDF	Features	Definition
Uniform		$f(x) = 1/(b - a)$
Triangular	Shape parameter c with $a \leq c \leq b$	$f(x) = 2(x - a)/(b - a)(c - a)$ if $a \leq x \leq c$ $f(x) = 2(b - x)/(b - a)(b - c)$ if $c \leq x \leq b$
Exponential	Location parameter γ Scale parameter λ	$f(x) = \lambda \exp[-\lambda (x - \gamma)]$
Normal	Mean value μ Standard deviation σ	$f(x) = \exp[-(x - \mu)^2/2\sigma^2]/\sigma(2\pi)^{1/2}$
Lognormal	Mean value of logarithms μ Standard deviation of logarithms σ	$f(x) = \exp[-(\ln(x) - \mu)^2/2\sigma^2]/(x\sigma(2\pi)^{1/2})$

2.3 Precision

Precision characterises the degree of mutual agreement among a series of individual measurements, values, or results (Coleman, 1995). An example of the precision in measurement of variable x is given in Figure 2.1 (Coleman, 1995).

Figure 2.3.1: Precision in measurement of variable x 

Source: Coleman (1995).

For a series of N individual assessments by a code of a variable $x(x_n^{code})$, the following criteria can be defined to perform a statistical comparison with an experimental result:

- 1) Mean value: $x^{code} = \frac{1}{N} \sum_{n \leq N} x_n^{code}$
- 2) Individual relative bias error: $\delta_n^{code} = \frac{x_n^{code} - x^{exp}}{x^{exp}}$
- 3) Mean relative bias error: $\delta^{code} = \frac{1}{N} \sum_{n \leq N} \delta_n^{code}$
- 4) Maximum bias error: $\epsilon^{code} = \max |\delta_n^{code}|$
- 5) Standard deviation: $\sigma^{code} = \sqrt{\frac{1}{N} \sum_{n \leq N} (x_n^{code} - x^{code})^2}$
- 6) Coverage ratio: the proportion of individual assessments among the series with a relative bias error lower than the experimental uncertainty ϵ^{exp} :

$$R^{code} = \frac{\text{card}\{\delta_n^{code} \text{ with } \delta_n^{code} \leq \epsilon^{exp}\}}{N}$$

2.4 Uncertainty

Uncertainty is an estimation of scatter in a measurement or in a result, usually determined with a certain level of confidence (often 95%) (Wheeler, 1996; Hochreiter, 2006). Considering a model producing output results as a function of “uncertain” input parameters, propagation of uncertainty (or propagation

of error) is the effect of the input uncertainties on the output results. In other words, this quantifies the variation of the results for a given variation (range and PDF) of input parameters. Mainly, the variables are measured in an experiment, and have uncertainties due to measurement limitations (e.g. instrument precision), which propagate to the results.

2.5 Sensitivity analysis

Sensitivity analysis (SA) is a study of how the response of a model (numerical or otherwise) can qualitatively or quantitatively be apportioned to different sources of input variations (Wheeler, 1996; Saltelli, 2000, 2004). SA is thus closely linked to uncertainty analysis (UA), which aims to quantify the overall uncertainty associated with the response as a result of uncertainties in the model input.

The mathematical model of a given phenomenon is defined by a series of equations, input factors, parameters and variables aimed to characterise the process being investigated. Input is subject to many sources of uncertainty including errors of measurement, absence of information and poor or partial understanding of the driving forces and mechanisms. The uncertainties impose a limit on the confidence in the response or output of the model. Further, models may have to cope with the natural intrinsic variability of the system, such as the occurrence of stochastic events. Good modelling practice requires that the modeller provide an evaluation of the confidence in the model, possibly assessing the uncertainties associated with the modelling process and with the outcome of the model itself. Therefore, the uncertainty and sensitivity analyses offer valid tools for characterising the uncertainties associated with the model and can be used to determine:

- the model resemblance with the process under study;
- the quality of model definition;
- the factors that mostly contribute to the output variability;
- the region in the space of input factors for which the model variation is maximum;
- the optimal or instability regions within the space of factors for use in a subsequent calibration study;
- the interactions between the factors.

The sensitivity analysis is popular in financial applications, risk analysis, signal processing and any area where models are developed. Sensitivity analysis can also be used in model-based policy assessment studies.

There are several possible procedures to perform uncertainty and sensitivity analyses. The most common sensitivity analysis is the sampling-based sensitivity. In the sampling-based sensitivity analysis the model is executed repeatedly for combinations of values sampled from the distribution (assumed known) of the input factors. In general, UA and SA are performed jointly by executing the model repeatedly for combination of factor values sampled with some probability distribution. The following steps can be listed:

- specify the target function and select the input of interest;
- assign a distribution function to the selected factors;
- generate a matrix of inputs with that distribution(s) through an appropriate design;
- evaluate the model and compute the distribution of the target function;
- select a method for assessing the influence or relative importance of each input factor on the target function.

2.6 Verification and validation

Verification and *validation* are defined as primary means to assess the accuracy and reliability of simulations (Roache, 1998; Mahaffy, 2010; Oberkampf, 2006). Oberkampf (2006) separates verification into two groups. The first is the *code verification* and the second is the *solution verification*. The code

verification was defined as an assessment of the reliability of the software coding. The solution verification deals with the numerical accuracy of the computational model. In the same paper, Oberkampf defined validation as a physical modelling accuracy of a computational simulation by comparing with experimental data. Briefly, *verification* is the process of ensuring that the controlling physical equations have been correctly translated into computer code or in the case of hand calculations, correctly incorporated into the calculation procedure. Validation is defined as the evidence that demonstrates that the selected code or calculation method is suitable for the specific analysis purpose. This includes the confirmation that the results from the verified model agree with the benchmarks (Ravenswaay, 2006).

Because verification and validation terms have elements similar to uncertainty and sensitivity analysis, it is possible to confuse the verification and validation with the uncertainty analysis. The BFBT benchmark team defined uncertainty analyses for void distribution and critical power, not verification and validation analyses. The participants are free to choose the model for their uncertainty and sensitivity analyses.

A review of UA and SA methodologies is provided in Appendix 1.

Chapter 3: Selection and characterisation of uncertainty input parameters for BFBT benchmark

3.1 Uncertainty input parameters for Exercises I-4 and II-3

Some of the possible input parameters for the uncertainty analysis are classified in the following groups:

- Boundary condition effects – hydraulic and thermal input variables as:
 - mass flow rate;
 - inlet fluid temperature (or inlet sub-cooling);
 - system pressure;
 - power (or outlet quality).
- Geometry effects – dimensions of the bundle components as:
 - diameter of the heated rod;
 - thickness of the cladding;
 - flow area of the sub-channel;
 - wetted perimeter of the sub-channel, etc.
- Modelling parameters used in the code as:
 - friction factors (single-phase factor, two-phase multiplier, heating corrector);
 - single-phase and two-phase heat transfer coefficients;
 - boiling/condensation and interfacial mass transfer factors;
 - turbulence and mixing coefficients;
 - void drift model parameters;
 - spacer loss coefficient.

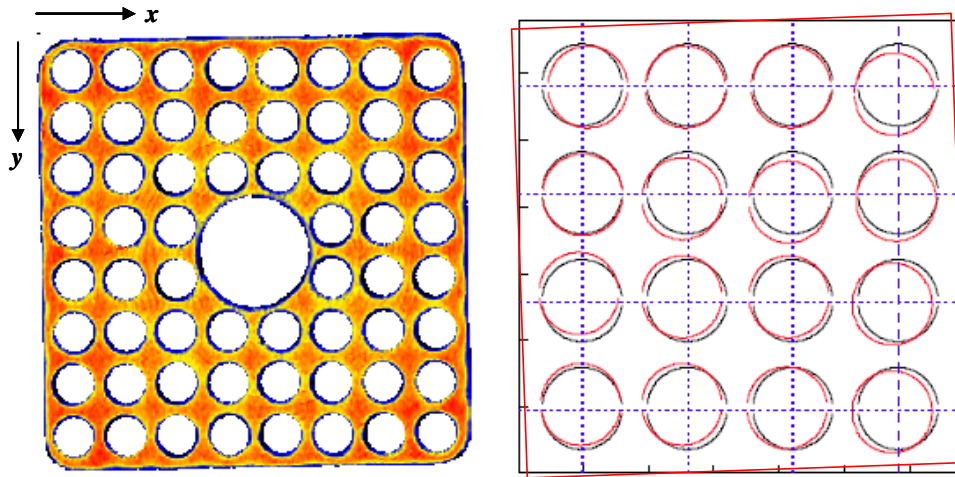
Each of the hydraulic and thermal input parameters is characterised by a range of experimental uncertainties that were determined by the experimental team (Table 3.1.1). These uncertainties must be related to a probability density function (PDF) (Glaeser, 2000). In order to extend and enrich the proposed sensitivity analysis, BFBT participants are encouraged to specify their own additional uncertainty parameters, especially modelling parameters (with accuracy range and related PDF) and present them to the benchmark team while submitting their results.

Table 3.1.1 provides the accuracies and PDF of measured variables (inlet temperature, mass flow rate, system pressure and bundle power).

As can be seen in Figure 3.1.1 the assembly walls are not quite horizontal or vertical. The deviation for the horizontal (W-E) or the vertical (N-S) is 4 pixels in each edge. The average deviation of rod centres from the design (in pixels) is shown to be about 1.5 pixels for both the x and y errors.

Table 3.1.1: Estimated accuracy and PDF of the main process parameters

Quantity	Accuracy range	PDF
System pressure	$\pm 1\%$	Normal
Mass flow rate	$\pm 1\%$	Normal
Power	$\pm 1.5\%$	Normal
Inlet fluid temperature	$\pm 1.5^\circ\text{C}$	Flat

Figure 3.1.1: Distortions of test assembly observed with fine-mesh void measurement

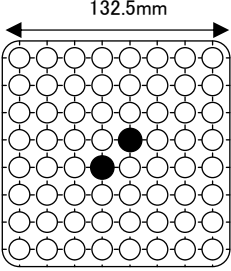
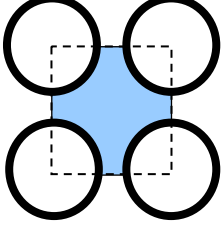
Based on the observation of the X-ray CT scan data (see Figure 3.1.1), one can make assumptions about the distortion for the heater pin and channel box, which can quantify the accuracy of the rod diameter due to manufacturing (1.5 pixels), the accuracy of the rod pitch (1.5 pixels) and the accuracy of the bundle inner width (4 pixels).

The US NRC developed the Phenomena Identification Ranking Table (PIRT) concept for assessing the relative importance of individual phenomena (models or correlations) involved in determining safety margins in operating reactors (Boyack, 1995; Holowach, 2006; Martin, 2005; US NRC, 1989, 1989a). The PIRT help to determine which phenomena are the most important for a given scenario. A group of experts at PSU developed PIRT tables to rank the most important phenomena that need to be accurately simulated for each uncertainty exercise – void distribution and critical power. Another independent group of experts reviewed these PIRT tables and the ranking of the phenomena and concurred or disagreed with the first group. The first group then resolved the differences. The PIRT-related information is provided in Appendix 2. The components of interest for the void distribution uncertainty exercise are the sub-channel void distribution and bundle average void fraction at the bundle exit. Tables A2.1 through A2.4 in Appendix 2 provide the PIRT tables for the void distribution. The components of interest for the critical power uncertainty exercise are the steady-state critical power and the dry-out elevation. Tables A2.5 through A2.8 in Appendix 2 provide the PIRT tables for the critical power.

3.2 Description of the elemental task

The elemental channel is a single sub-channel defined by four adjusting rods in a fuel assembly. The cross-section of the elemental channel is a square with each side equal to the rod pitch. The reference of the elemental channel is assembly type 0-1. Table 3.2.1 provides the geometry and power shape data for the elemental channel.

Table 3.2.1: Geometry and power shape of the elemental channel

Item	Data	
Assembly		
	0-1	Elemental channel
Simulated fuel assembly type	8 × 8	
Number of heated rods	62	1
Number of water rods	2	0
Heated rods outer diameter (mm)	12.3	
Heated rods pitch (mm)	16.2	
Axial heated length (mm)	3 708	
Water rods outer diameter (mm)	15.0	–
Channel box inner width (mm)	132.5	–
Channel box corner radius (mm)	8.0	–
Inchannel flow area (mm ²)	9 781	143.6
Spacer type	Grid	Grid and ferrule
Number of spacers	7	
Spacer pressure loss coefficients	1.2	
Spacer location (mm)	455, 967, 1 479, 1 991, 2 503, 3 015, 3 527 (distance from bottom of heated length to spacer bottom face)	
Radial power shape	Uniform	
Axial power shape	Uniform	

The void fraction in a sub-channel ij at the bundle quality x_e can be separated as:

$$\alpha^{ij}(x_e) = \alpha(x_e) + \alpha_{cf}^{ij}(x_e) \quad (3.1)$$

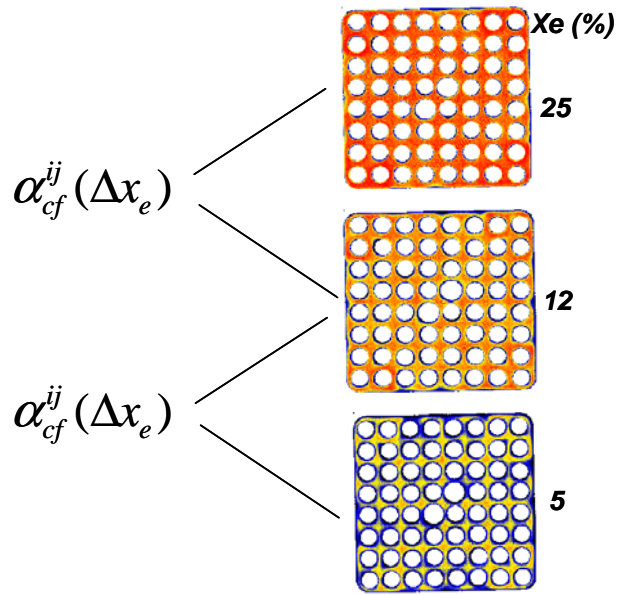
where $\alpha^{ij}(x_e)$ is the void fraction in sub-channel ij at the bundle quality x_e , $\alpha(x_e)$ is the void fraction in the elemental channel at quality x_e and $\alpha_{cf}^{ij}(x_e)$ is the void fraction due to cross-flow into sub-channel ij at the bundle quality x_e .

Then, we obtain:

$$\alpha_{cf}^{ij}(x_e) = \alpha^{ij}(x_e) - \alpha(x_e) \quad (3.2)$$

Actually, the value of $\alpha_{cf}^{ij}(x_e)$ shall be defined for the deviation of the quality x_e . There are three different bundle quality cases in the benchmark exercise. By taking the deviation of Eq. (3.2), the value of $\alpha_{cf}^{ij}(x_e)$ will be quantified. An image of this process is shown in Figure 3.2.1.

Figure 3.2.1: Image to quantify the cross-flow



Chapter 4: Suggested methods to be used in the uncertainty exercises of BFBT benchmark

Exercise 4 of Phase I and Exercise 3 of Phase II of the BFBT benchmark will be performed in two steps.

The first step is a standard type of accuracy analysis or global sensitivity analysis, where the total overall code predictions are compared to the experimental data.

The second step is an in-depth uncertainty analysis or local propagation of uncertainty of the boundary conditions, geometry effects and models/correlations of a given computer code by using the experimental data.

4.1 Step 1: Accuracy analysis

In Step 1 comparisons will be performed between the computer code prediction of the given quantity (void fraction/critical power) and its measured value.

An approach similar to the accuracy analyses of the Duke Power Company thermal-hydraulic statistical core design methodology is proposed (Duke, 1996). In this approach, the predicted parameter is compared with the measured one as shown in Figure 4.1.1 and Figure 4.1.2. In Figure 4.1.2, the parameter to be compared is the ratio of the predicted (P) void fraction to the measured (M) void fraction on a sub-channel basis. The P/M ratio can be used to assess the accuracy and degree of agreement of the analysis model with the data over a range of independent variables as pressure, mass flow, quality and inlet sub-cooling.

Figure 4.1.1: Example of predicted critical power versus measured critical power

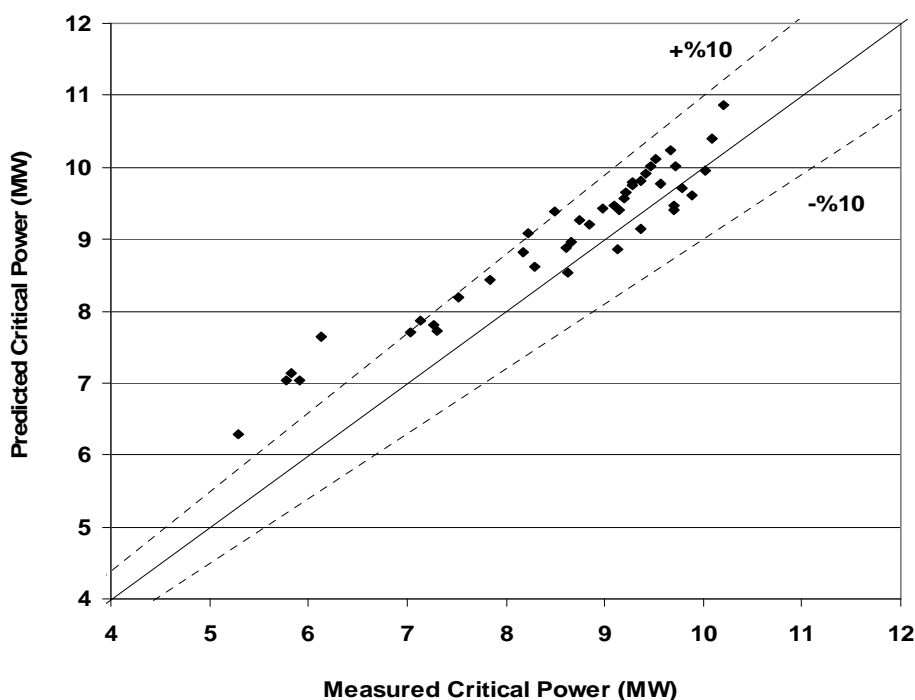
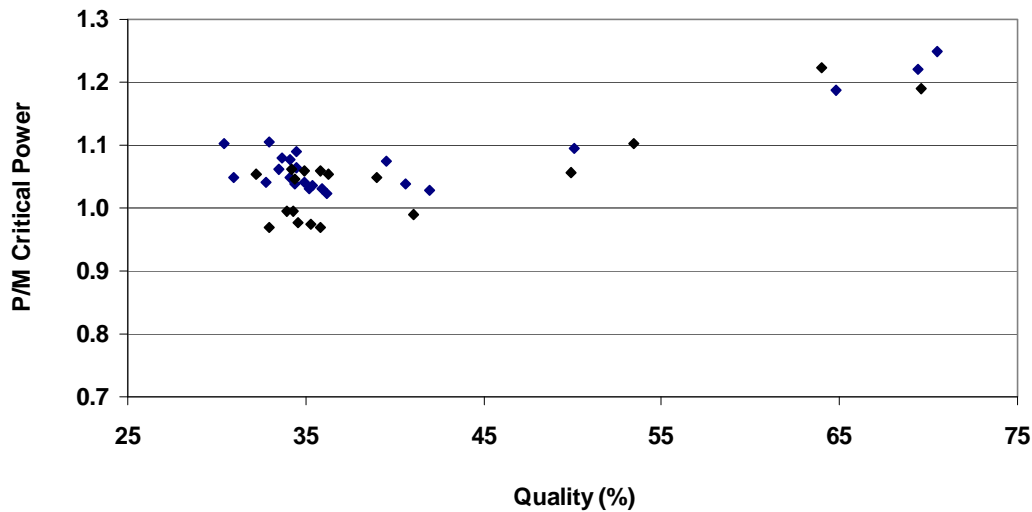


Figure 4.1.2: Example of predicted to measured critical power versus quality

Several meaningful comparisons can be obtained by comparing the measured void fraction/critical power to the predicted void fraction/critical power and plotting the P/M ratios. For example, P/M sub-channel void fraction histogram plots can be developed for the different sub-channel types. These plots will indicate a potential bias in the computer codes' capability to model different geometrical configurations and the related local flow patterns.

The other plots of interest are the P/M plots as a function of the test independent variables as pressure, mass flow, quality and inlet sub-cooling. One example is shown in Figure 4.1.2, where the P/M critical power ratio is plotted as a function of the exit quality. These types of plots will indicate a possible bias with the independent variables and will indicate potential deficiencies of the different computer code models.

In the Step 1 analyses in order to access the importance of a given input parameter on the code predictions, one parameter changes while the rest remain constant.

4.2 Step 2: Uncertainty analysis

Step 2 is devoted to uncertainty analysis of the void fraction and critical power predictions. This step will fulfil two main objectives: to assess the actual accuracy of thermal-hydraulic models for void fraction/critical power predictions in rod bundles and to compare the available methods for uncertainty analysis in thermal-hydraulics. There are several stages in the uncertainty analysis:

- 1) Analysis of experimental data and its sources of uncertainty (boundary conditions, geometry, measurement technique).
- 2) Selection of the most (or potential) sensitive parameters in the physical models and/or in the input data (*parametric identification*).
- 3) Propagation of the selected uncertainties from Part 2 through the calculations; this may require a large number of calculations using PDF (sampling) for the selected model parameters used in the code.
- 4) Analysis of the computational results (sub-channel data of void fraction for Phase I, Exercise 4 or overall critical power for Phase II, Exercise 3) with the criteria given in Chapter 2:
 - to assess the code precision with the sample-averaged bias error;
 - to assess the code uncertainty with the sample-averaged standard deviation;
 - to assess the code reliability with the proportion of specimens among the sample with a bias error lower than the experimental uncertainty.

The uncertainty parameters in the experiments with their characteristics are of two types:

- *Input uncertainties* – related to the geometry (*e.g.* fuel rod diameter) and the boundary conditions (temperature, mass flow, pressure and power) of the test section.
- *Output uncertainties* – related to the measurements of sub-channel void fractions and critical power.

The uncertainties of the input parameters, with their probability density functions, are indicated in Chapter 3. The participants are requested to propagate these uncertainties through the codes, possibly combined with uncertain parameters of the physical models as in Stages 2 and 3 above, and perform the void fraction and critical power calculations associated with the uncertainty. It is recommended to propagate input uncertainties on all parameters at once in order to assess cross-term effects. Sensitivity analysis on sampling technique or sampling size is possible to assess the effect on statistical results such as standard deviation.

The uncertainty of measured void fraction on different spatial levels is given in Table 4.2.1.

Table 4.2.1: Estimated accuracy of void distribution measurements

Quantity	Accuracy
X-ray CT scanner	
Local void fraction	8%
Sub-channel void fraction	3%
Cross-sectional void fraction	2%
X-ray densitometer chordal void	
Fraction	2%

In Table 4.2.1, the provided accuracy values of measured void fraction are the absolute accuracy in measurement data. According to Inoue (1995), the accuracy of the void fraction measurements with X-ray CT scanner depends on: i) the photon statistics of the X-ray source; ii) the detector non-linearity; iii) the accuracy of fluid condition (temperature and pressure) measurements. The accuracy on different levels – pixel, sub-channel, bundle and etc., has been logically estimated as a sum of the effects on measurements with these error elements.

Further, the cross-sectional accuracy was confirmed by the calibration test. The void pattern in the bubbly and annular flow was simulated with acrylic and water. The cross-sectional void fraction for reference was calculated geometrically. The deviation of the measured cross-sectional void fraction from the reference value was evaluated. The logically estimated accuracy for the cross-sectional void fraction is 2%. The calibrated value meets the estimated accuracy. In this discussion, the deviation was dealt with an absolute value.

Chapter 5: Selection of the exercise cases from the BFBT database

The BFBT benchmark team selected the BFBT data sets for the uncertainty analysis exercises of the void distribution and critical power benchmark phases. The selections of the cases for the accuracy analysis (Step 1) and for the uncertainty analysis (Step 2) were performed separately and therefore, the number of the selected cases for both steps is different. Another difference is the selected bundle type for void distribution accuracy/sensitivity analyses: for accuracy analysis (Step 1) bundle type 1 was selected, while for the uncertainty analyses (Step 2) bundle type 4 was selected. The reason for this difference is the pressure drop measured data collected for bundle type 4 that can be used to perform optimisation/initialisation of the uncertainty analysis.

The selected cases for the accuracy analysis step are discussed in Sections 5.1 and 5.2 respectively.

The selected cases for the uncertainty analysis step are discussed in Sections 5.3 and 5.4 respectively.

The selected cases for the elemental task are given in Section 5.5.

5.1 Selected cases for accuracy analysis of void distribution

To cover a wide range of operating conditions with a limited number of cases from the BFBT database, a sampling was performed by the benchmark team and a list of eleven experimental cases was defined (see Table 5.1.1). Assembly type 1 was selected for this exercise. A detailed description of assembly type 1 is given in NEA (2006). Briefly, it is a standard 8×8 rod bundle that includes two central water rods and has a non-uniform radial power distribution and a cosine axial power profile.

Table 5.1.1: Selected cases for accuracy analysis in Exercise 4 of Phase I

Analysis number	Pressure	Flow rate	Quality	Inlet sub-cooling	First selected case	Second selected case	Third selected case	Fourth selected case
1	Constant	Constant	Constant	Changing	1071-55	1071-62	–	–
2	Constant	Constant	Changing	Constant	1071-53	1071-55	1071-58	1071-61
3	Constant	Changing	Constant	Constant	1071-34	1071-40	1071-55	1071-65
4	Changing	Constant	Constant	Constant	1071-12	1071-27	1071-55	1071-82

The set of the three test cases 1071-55, 1071-58 and 1071-61 already selected for Exercise 1 of Phase I was expanded with eight additional test cases to be used for the accuracy analysis step. These are test cases 1071-12, 1071-27, 1071-34, 1071-40, 1071-53, 1071-65, 1071-62 and 1071-82.

The selected cases are summarised in Tables 5.1.2 and 5.1.3. The values of sub-cooling in Table 5.1.2 are approximate values and the real sub-cooling during the experiments varied around these approximate values.

Table 5.1.2: Test matrix of selected cases for Exercise 4 of Phase I

Assembly	Pressure (MPa)	Inlet sub-cooling (kJ/kg)	Flow rate (t/h)	Exit quality (%)					
				2	5	8	12	18	25
1	1.0	50.2	55	X	E4	X	X	–	–
1	3.9	50.2	55	X	E4	X	X	X	X
1	7.2	50.2	10	X	E4	X	X	X	X
1	7.2	50.2	20	X	E4	X	X	X	X
1	7.2	50.2	55	E4,W	E4	W	E4	W	E4
1	7.2	50.2	70	X	E4	X	X	X	–
1	7.2	126.0	55	E4	X	–	X	–	–
1	8.6	50.2	55	X	E4	X	X	W	–

X: Test case, W: Duplicated test case, E4: Exercise 4 case.

Table 5.1.3: Test numbers of selected cases for Exercise 4 of Phase I

Test no.	Assembly	Pressure (MPa)	Flow rate (t/h)	Inlet sub-cooling (kJ/kg)	Power (MW)	Exit quality (%)	Exercise cases
1071-12	1	1.016	54.92	56.2	2.32	5.0	E4
1071-27	1	3.944	54.71	50.7	2.09	5.0	E4
1071-34	1	7.164	10.22	49.5	0.36	5.0	E4
1071-40	1	7.161	20.00	63.6	0.70	5.0	E4
1071-53	1	7.185	54.58	52.2	1.23	2.0	E4
1071-55	1	7.190	54.60	52.8	1.92	4.9	E4
1071-58	1	7.160	55.10	50.3	3.52	11.9	E4
1071-61	1	7.200	54.70	51.8	6.48	25.1	E4
1071-62	1	7.147	54.85	124.6	3.07	5.0	E4
1071-65	1	7.195	69.49	53.9	2.45	5.0	E4
1071-82	1	8.633	54.69	51.7	1.85	5.0	E4

5.2 Selected cases for accuracy analysis of critical power

Similar to the approach adopted in the previous section, to cover a wide range of operating conditions with a limited number of cases from the BFBT database, a sampling was performed by the benchmark team and a list of nine experimental cases was defined (see Table 5.2.1). Assembly C2A (NEA, 2006) was selected for this exercise. Assembly C2A is a “high burn-up” rod bundle that includes one central large water rod and has a non-uniform radial power distribution and a cosine axial power profile.

Tables 5.2.2 and 5.2.3 show, respectively, the test matrix and experimental conditions of selected cases. The values of sub-cooling in Table 5.2.2 are approximate values and the real sub-cooling during the experiments was varying around these approximate values.

Table 5.2.1: Selected cases for Exercise 3 of Phase II

Analysis number	Pressure	Flow rate	Inlet sub-cooling	First selected case	Second selected case	Third selected case	Fourth selected case
1	Constant	Constant	Changing	SA610503	SA610600	SA610700	SA610900
2	Constant	Changing	Constant	SA612500	SA605500	SA607500	SA610503
3	Changing	Constant	Constant	SA510500	SA610503	SA810501	–

Table 5.2.2: Test matrix of selected cases for Exercise 3 of Phase II

Assembly	Pressure (MPa)	Flow rate (t/h)	Inlet sub-cooling (kJ/kg)				No. of data		
			25	50	84	104		126	
C2A	5.5	20	X	W	X	–	X	20	
		45	X	X	X	–	X		
		55	W	E3, W	W	–	X		
		65	X	X	X	–	X		
	7.2	10	X	X	X	X	X	35	
		20	X	E3, W	X	X	X		
		30	X	E3	X	X	X		
		45	X	X	X	X	X		
		55	E3, W	E3, W	E3	E3, W	X		
		60	X	X	X	X	X		
	8.6	65	X	E3	X	X	X	20	
		20	X	W	X	–	X		
		45	X	X	X	–	X		
		55	W	E3, W	W	–	X		
			65	X	X	X	–	X	

X: Test case, W: Duplicated test case, E3: Exercise 3 case.

Table 5.2.3: Experimental conditions of selected cases for Exercise 3 of Phase II

Test no.	Outlet pressure (MPa)	Flow rate (t/h)	Inlet sub-cooling (kJ/kg)	Experimental cases
SA510500	5.48	55.06	56.41	Duplicated test, E1, E3
SA605500	7.16	20.09	50.55	Duplicated test, E1, E3
SA607500	7.13	30.02	48.35	E1, E3
SA610503	7.17	55.20	59.39	Duplicated test, E1, E3
SA610600	7.18	55.05	89.53	E1, E3
SA610700	7.13	55.20	107.61	Duplicated test, E1, E3
SA610900	7.27	55.10	37.73	Duplicated test, E1, E3
SA612500	7.16	65.36	55.66	E1, E3
SA810501	8.62	55.15	54.89	Duplicated test, E1, E3

5.3 Selected cases for uncertainty analysis of void distribution

NUPEC has used different bundle types for various measurements. The bundle types used for the steady-state void distribution, steady-state critical power, steady-state single- and two-phase pressure drop measurements are summarised in Table 5.3.1. An optimisation of the code is necessary before the uncertainty analyses are carried out. For example, an optimisation can be performed in order to determine the axial node size. Also, the pressure drop data can be used for the optimisation purposes. As already discussed, in the BFBT database, the pressure drop data was collected for assembly type C2A, which is a sub-type of assembly type 4. Therefore, assembly types 4 and C2A were selected, respectively, for the uncertainty analyses of the steady-state void distribution and for the uncertainty analyses of the steady-state critical power.

Four experimental cases were selected that are considered covering the BFBT database for the purpose of uncertainty analyses of the steady-state void distribution. Table 5.3.2 summarises the selected cases.

Table 5.3.1: The bundle types used in the BFBT measurements

Phase	Exercises		Assembly type
Void distribution	Steady-state sub-channel		<u>0-1</u>
			<u>0-2</u>
			<u>0-3</u>
			<u>1</u>
			<u>2</u>
			<u>3</u>
			<u>4</u>
	Steady-state microscopic		0-1
			0-2
			0-3
			1
			2
			3
			4
	Transient macroscopic	4	
Critical power	Steady-state	Pressure drop	C2A (single-phase)
			C2A (for two-phase)
	Critical power		<u>C2A</u>
			<u>C2B</u>
	Transient	Critical power	<u>C3</u>
		C2A	

Table 5.3.2: Selected cases for uncertainty analysis of void distribution

Test case	Void fraction	Pressure (MPa)	Flow rate (t/h)	Inlet sub-cooling (kJ/kg)	Outlet quality (%)
Test 4101-02	57.1	0.994	10.12	53.3	0.32
Test 4101-13	86.8	1.224	55.01	92.5	4.46
Test 4101-69	18.2	8.638	10.08	52.5	0.23
Test 4101-86	69.8	8.705	54.59	54.2	4.62

5.4 Selected cases for uncertainty analysis of critical power

Four experimental cases were selected that are considered covering the BFBT database for the purpose of uncertainty analyses of the steady-state critical power. Table 5.4.1 summarises the selected cases.

Table 5.4.1: Selected cases for uncertainty analysis of critical power

Test case	Pressure (MPa)	Flow rate (t/h)	Inlet sub-cooling (kJ/kg)	Critical power (MW)	Dry-out rod number	Elevation	Angle
SA603901	7.18	10.01	25.82	3.2	8	A	330
SA505900	5.49	20.14	26.04	5.98	4	A	240
SA812800	8.67	65.27	135.52	8.9	8	B	330
SA512800	5.5	65.52	133.75	11.09	53	A	150

5.5 Selected cases for elemental task

The reference test matrix and test numbers for the elemental task are shown in Tables 5.5.1 and 5.5.2, respectively, where the cases are denoted with T1 and T2. Table 5.5.3 provides the boundary conditions for the Sub-tasks 1 and 2 of the elemental task. The power and the flow rate of the reference cases are divided by the ratio of the number of rods and the flow area between the assembly type 0-1 and the elemental channel. In Sub-task 2, the power shall be increased until the dry-out occurs. If the spacer effect is modelled in Sub-task 2, both spacer types, grid and ferrule, have to be considered.

Table 5.5.1: Reference test matrix for elemental task

Assembly	Pressure (MPa)	Inlet sub-cooling (kJ/kg)	Flow rate (t/h)	Exit quality (%)					
				2	5	8	12	18	25
0-1	7.2	50.2	10	X	X	X	X	X	X
			20	X	X	X	X	X	X
			30	X	X	X	X	X	X
			55	W	T1	W	T1	W	T1, T2
			70	X	X	X	X	X	–

X: Test case, W: Duplicated test case, T1: Task 1 reference case, T2: Task 2 reference case.

Table 5.5.2: Reference test numbers for the elemental task

Test no.	Assembly	Pressure (MPa)	Flow rate (t/h)	Inlet sub-cooling (kJ/kg)	Power (MW)	Exit quality (%)	Task cases
0011-55	0-1	7.180	54.03	52.6	1.90	5.0	T1
0011-58	0-1	7.172	54.90	51.0	3.51	12.0	T1
0011-61	0-1	7.210	54.79	50.9	6.44	24.9	T1, T2

Table 5.5.3: Boundary conditions for the elemental task

Reference test no.	Pressure (MPa)	Flow rate (kg/h)	Inlet sub-cooling (kJ/kg)	Power (kW)	Task cases
0011-55	7.180	772.2	52.6	30.65	T1
0011-58	7.172	806.0	51.0	56.61	T1
0011-61	7.210	804.4	50.9	103.87	T1, T2

Chapter 6: Requested output

6.1 Introduction

Participants should provide the output information with the given requirements:

- discussion of the uncertainty approaches used;
- results should be presented in electronic format;
- all output should be in SI units.

Templates of requested output data for each exercise will be provided by the benchmark team.

The Pennsylvania State University will:

- provide code-to-code comparisons for different submittals;
- provide overall conclusions on current code capabilities.

6.2 Requested output for Exercise 4 of Phase I

The requested output format for Exercise 4 of Phase I is given in this section.

Step 1: Accuracy analysis of steady-state void distribution

Using the deterministic values for input parameters, the “deterministic void distribution” for each selected case should be calculated and submitted as a 9×9 matrix (Table 6.2.1).

Table 6.2.1: Calculated void distribution from deterministic input parameters

y/x	1	2	3	4	5	6	7	8	9
1	xx	xx	xx	xx	xx	xx	xx	xx	xx
2	xx	xx	xx	xx	xx	xx	xx	xx	xx
3	xx	xx	xx	xx	xx	xx	xx	xx	xx
4	xx	xx	xx	xx	xx	xx	xx	xx	xx
5	xx	xx	xx	xx	xx	xx	xx	xx	xx
6	xx	xx	xx	xx	xx	xx	xx	xx	xx
7	xx	xx	xx	xx	xx	xx	xx	xx	xx
8	xx	xx	xx	xx	xx	xx	xx	xx	xx
9	xx	xx	xx	xx	xx	xx	xx	xx	xx

Step 2: Uncertainty analysis of steady-state void distribution

For each selected case, the following outputs should be submitted as a 9×9 matrix (cf. definitions in Chapter 2):

- sample-averaged void distribution;
- sample-averaged bias error;
- maximum bias error;
- sample-averaged standard deviation;
- coverage ratio with epsilon $\epsilon^{\text{exp}} = (3\%/\alpha^{\text{exp}})$ at the sub-channel scale.¹

A questionnaire should be filled in to present the sampling technique and size used for this uncertainty analysis. Since the participants can propagate their own additional uncertain parameters, especially modelling parameters, they should clearly indicate the associated range of variation and the PDF considered for each extra input parameter.

6.3 Requested output for Exercise 3 of Phase II

The requested output format for Exercise 3 of Phase II is given in this section.

Step 1: Accuracy analysis of steady-state critical power

Using the deterministic values for input parameters, the “deterministic critical power” for each selected case should be calculated and submitted as a 9×9 matrix (Table 6.3.1).

Table 6.3.1: Calculated critical power from deterministic input parameters

y/x	1	2	3	4	5	6	7	8	9
1	XX	XX	XX	XX	XX	XX	XX	XX	XX
2	XX	XX	XX	XX	XX	XX	XX	XX	XX
3	XX	XX	XX	XX	XX	XX	XX	XX	XX
4	XX	XX	XX	XX	XX	XX	XX	XX	XX
5	XX	XX	XX	XX	XX	XX	XX	XX	XX
6	XX	XX	XX	XX	XX	XX	XX	XX	XX
7	XX	XX	XX	XX	XX	XX	XX	XX	XX
8	XX	XX	XX	XX	XX	XX	XX	XX	XX
9	XX	XX	XX	XX	XX	XX	XX	XX	XX

Step 2: Uncertainty analysis of steady-state critical power

In this step, uncertainty analyses of critical power have to be performed for the critical power value, the dry-out elevation, the dry-out rod number and the dry-out angle. Because of the difficulties to statistically handle and analyse the localisation aspects, it is decided to focus solely on the critical power value.

1. See Chapter 2: ϵ^{exp} is the relative error while $\Delta\alpha^{\text{exp}} = 3\%$ is the absolute error on void fraction data at the sub-channel scale.

Participants should submit their results by using the format given in Table 6.3.2.

Table 6.3.2: The calculated critical power uncertainty output format

Test number	Sample-averaged critical power	Sample-averaged bias error	Sample-maximum bias error	Sample-averaged standard deviation	Coverage ratio with a bias error lower than the experimental uncertainty ($\epsilon^{\text{exp}} = 1.5\%$)
XX	XX	XX	XX	XX	XX
XX	XX	XX	XX	XX	XX

6.4 Requested output for elemental task

The following comparisons will be performed in the elemental task:

- code-to-code comparisons on the analytical model for different submittals;
- code-to-code comparisons on the analytical results for different submittals.

Sub-task 1: Void fraction in the elemental channel benchmark

Analytical model:

- basic field thermal-hydraulics;
- sub-cooled boiling model;
- flow regime map;
- transfer between phases (mass, momentum and energy);
- transfer between fluid and wall (momentum and energy);
- spacer effect on pressure drop;
- nodalisation mesh.

Analytical results:

- axial profile of equilibrium quality (x_e);
- axial profile of flow quality (x);
- axial profile of void fraction (α);
- axial profile of liquid velocity;
- axial profile of vapour velocity;
- axial profile of pressure difference from outlet;
- relation of equilibrium quality and void fraction (see Figure 6.4.1).

Sub-task 2: Critical power in the elemental channel benchmark

Analytical model:

- onset of annular-mist flow;
- entrainment at the onset of annular-mist flow;
- droplet entrainment;
- droplet deposition;

- spacer effect on droplets;
- film thickness at dry-out;
- nodalisation mesh.

Analytical results:

- axial profile of liquid film flow rate;
- axial profile of entrained droplet flow rate;
- axial profile of flow quality;
- axial profile of entraining droplet mass flux;
- axial profile of depositing droplet mass flux;
- critical power.

Figure 6.4.1: Example of relation between equilibrium quality and void fraction

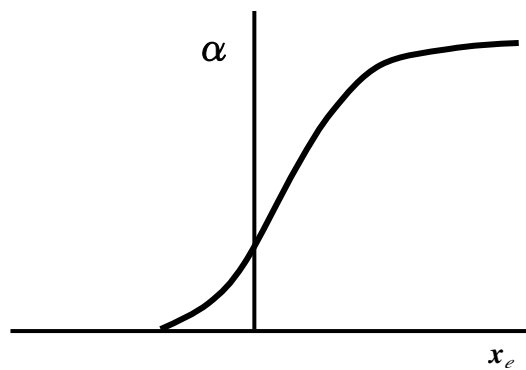
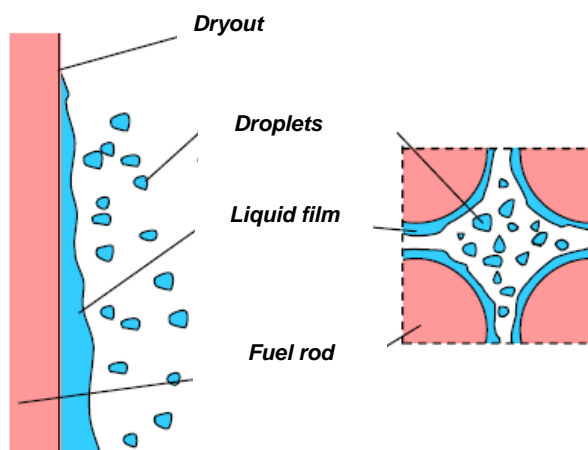


Figure 6.4.2: Structure of annular-mist flow



Chapter 7: Conclusions

The objective of the second volume of the BFBT specification is to provide the participants with information on the uncertainty and sensitivity analysis of void distribution and critical power. In order to reduce the amount of work, to make the analysis more precise and to avoid confusion when comparing the results of participants, specific test cases of the BFBT database were selected out for the OECD/NRC BFBT uncertainty benchmark exercises.

Exercise 4 of Phase I is devoted to uncertainty analyses of the void distribution predictions. The BFBT benchmark provides an opportunity to apply techniques of uncertainty analyses and to assess the accuracy of two-phase flows models. The steady-state void fraction predictions can be used to analyse these uncertainties and their propagation in the thermal-hydraulic models. The test cases for this exercise include some of the test cases of Exercise 1 of Phase I plus some additional test cases.

Exercise 3 of Phase II is devoted to uncertainty analyses of the critical power predictions. The goal of Exercise II-3 is to find the critical power uncertainties of the thermal-hydraulic codes using the BFBT benchmark database. This exercise provides the possibility of performing sensitivity/uncertainty analyses of the droplet deposition, liquid film entrainment, and spacer grid models and their impact on the codes' capabilities of predicting critical power.

References

- Adomian, G. (1980), *Stochastic System Analysis*, pp. 1-17, Academic Press, New York.
- Aydogan, F., et al. (2007), "Phenomena Identification Ranking Table for BWR Steady State Critical Power", *Nureth-12 International Conference* (255).
- Aydogan, F., et al. (2007a), "Phenomena Identification Ranking Table for BWR Steady State Void Distribution", *Nureth-12 International Conference* (254).
- Boyack, B. (1995), *AP600 Large-break Loss-of-coolant Accident Phenomena Identification and Ranking Tabulation*, LA-UR-95-2718, Los Alamos National Laboratory.
- Coleman, H.W., W.G. Steele (1995), "Engineering Application of Experimental Uncertainty Analysis", *AIAA Journal*, Vol. 33, No. 10, pp. 1888-1896.
- Doughtery, E.P., H. Rabitz (1979), "A Computational Algorithm for the Green's Function Method of Sensitivity Analysis in Chemical Kinetics", *International Journal of Chemical Kinetics*, 11, 1237-1249.
- Doughtery, E.P., J.T. Hwang, H. Rabitz (1979a), "Further Developments and Applications of the Green's Function Method of Sensitivity Analysis in Chemical Kinetics", *International Journal of Chemical Kinetics*, 71 (4), 1794-1808.
- Duke Power Company (1996), *Duke Power Company Thermal-hydraulic Statistical Core Design Methodology, BWU-Z CHF Correlation*.
- Dunker, A.M. (1984), "The Decoupled Direct Method for Calculating Sensitivity Coefficients in Chemical Kinetics", *Journal of Chemical Physics*, 81 (5), 2385-2393.
- Glaeser, H.G. (2000), "Uncertainty Evaluation of Thermal-hydraulic Code Results", *International Meeting on "Best-estimate" Methods in Nuclear Installation Safety Analysis*.
- Hochreiter, L.E. (2006), "Thermal-hydraulics Uncertainties as Applied to DNB Analysis and Best-estimated LOCA Calculations", *ACE Uncertainty Workshop*, North Carolina State University.
- Holowach, M.J. (2000), *The Development of a Reflood Heat Transfer Computational Package For Small Hydraulic Diameter Geometries*, MS Thesis, The Pennsylvania State University.
- Inoue, A., et al. (1995), "Void Fraction Distribution in BWR Fuel Assembly and Evaluation of Sub-channel Code", *Journal of Nuclear Science and Technology*, July.
- Isukapalli, S.S. (1999), *Uncertainty Analysis of Transport-transformation Models*, PhD Thesis, Rutgers, The State University of New Jersey.
- Mahaffy, John (2010), *Verification and Validation website*, accessed 10 February 2010, www.personal.psu.edu/faculty/j/h/jhm/470/lectures/VandV/VandV.html.
- Martin, R.P., L.D. O'Dell (2005), "AREVA's Realistic Large Break LOCA Analysis Methodology", *Nuclear Engineering and Design*, 235, 1713-1725.
- Nuclear Energy Agency (NEA) (1997), *Report of Uncertainty Analysis Methods Study for Advanced Best Estimate Thermal Hydraulic Code Applications*, NEA/GSNI/R(97)35, OECD/NEA, Paris.
- NEA (2006), *NUPEC BWR Full-size Fine-mesh Bundle Test (BFBT) Benchmark, Volume I: Specifications*, NEA/NSC/DOC(2005)5, OECD/NEA, Paris.

- Oberkampf, W.L., T.G. Trucano (2006), "Design of and Comparisons with Verification and Validation Benchmarks", *Proceedings of the Meeting on Benchmarking of CFD Codes for Application to Nuclear Reactor Safety (CFD4NRS)*, Garching (Munich), Germany, 5-7 September, accessed 11 February 2009, www.nea.fr/html/nsd/reports/2007/nea6298/invited.html.
- Prokopakis, G.J. (1993), "Decoupled Direct Method for the Solution of Ordinary Boundary Value Problems", *Applied Mathematical Modelling*, 17 (9), 499-503.
- Ravenswaay, Jan P., et al. (2006), "Verification and Validation of the HTGR Systems CFD Code Flownex", *Nuclear Engineering Design*, Vol. 236, Issues 5-6, March, pp. 491-501.
- Roache, P.J. (1998), *Verification and Validation in Computational Science and Engineering*, Hermosa Publishers, pp. 403-412.
- Roselle, S.J. (1994), "Effects of Biogenic Emission Uncertainties on Regional Photochemical Modeling of Control Strategies", *Atmospheric Environment*, 28 (10), 1757-1772.
- Saltelli, A., K. Chan, E.M. Scott (2000), *Sensitivity Analysis*, Wiley.
- Saltelli, A., et al. (2004), *Sensitivity Analysis in Practice. A Guide to Assessing Scientific Models*, John Wiley & Sons.
- Sistla, G., S.T. Rao, J. Godowitch (1991), "Sensitivity Analysis of a Nested Ozone Air Quality Model", *Proceedings of the AMS/AWMA Joint Conference on Applications of Air Pollution Modeling and its Applications*, New Orleans, LA.
- Tatang, M.A. (1992), *Combined Stochastic and Deterministic Approach in Solving Stochastic Differential Equations*, MS Thesis, Carnegie Mellon University.
- Tomović, R., M. Vukobratović (1972), *General Sensitivity Theory*, Elsevier, New York.
- US Nuclear Regulatory Commission (US NRC) (1989), "Best Estimate Calculations of Emergency Core Cooling Performance", *Regulatory Guide 1.157 (Task RS 701-4)*.
- US NRC (1989a), *Quantifying Reactor Safety Margins*, NUREG/CR-5249.
- Vanderperk, M. (1997), "Effect of Model Structure on the Accuracy and Uncertainty of Results from Water Quality Models", *Hydrological Processes*, 11 (3), 227-239.
- Vieux, B.E., B. Needham (1993), "Nonpoint-pollution Model Sensitivity to Grid-cell Size", *Journal of Water Resources Planning & Management-ASCE*, 119 (2), 141-157.
- Villadsen, J., M.L. Michelsen (1978), *Solution of Differential Equation Models by Polynomial Approximation*, Prentice-Hall, Englewood Cliffs, New Jersey.
- Wheeler, A.J., A.R. Ganji (1996), *Introduction to Nuclear Engineering Experimentation*, Prentice Hall.
- Wikipedia (2010), Sensitivity Analysis webpage, accessed 12 February 2010, http://en.wikipedia.org/wiki/Sensitivity_analysis.

Appendix 1: Uncertainty and sensitivity analysis methods

Uncertainty analysis (UA) and sensitivity analysis (SA) can be performed by several possible procedures, such as sampling methods, sensitivity testing, analytical methods and computer algebra-based methods (Isukapalli, 1999). In this chapter, these methods are defined with references given.

A1.1 Sampling methods

Some of the most common sensitivity analysis methods are the sampling-based methods (Wikipedia, 2010). These methods do not require modifications in the model equations.

Some of the sampling methods are listed below:

- Fourier Amplitude Sensitivity Test (FAST) methods;
- Monte Carlo and Latin Hypercube sampling methods;
- reliability-based methods.

Sampling methods are executed repeatedly for combinations of values sampled from the distribution (assumed known) of the input factors in this method.

For the combination of factor values sampled with some probability distribution, uncertainty and sensitivity analyses are performed jointly by executing the model repeatedly. The following steps can be listed:

- specify the target function (the function on which the uncertainty analysis will be applied) and select the input of interest;
- appoint a PDF to the selected factors;
- generate a matrix of inputs with that PDF;
- evaluate the model and compute the distribution of the target function;
- select and run a method in order to assess the influence or relative importance of each input factor on the target function.

A1.2 Sensitivity testing methods on models

The sensitivity testing method is run for a set of sample points with straightforward changes in the model structure. The model structure or parameters of the model are changed in this analysis method. Measuring the robustness of the model is the target of sensitivity testing methods by testing whether the model response to changes significantly after changing the model parameters or/and structural formulation of the model. Roselle (1994), Sistla (1991), Vieux (1993) and Vanderperk (1997) used this approach for different applications, such as sensitivity analysis.

Even though these sensitivity methods give information regarding the change of the model or the parameters in the model, detailed uncertainty information cannot be obtained.

A1.3 Analytical methods for UA/SA

The analytical methods for UA/SA involve either the reformulation of the original model using stochastic algebraic/differential equations or differentiation of the model equations and subsequent solution of a set of auxiliary sensitivity equations.

Some of the analytical methods are listed below:

- coupled and decoupled direct methods;
- spectral-based stochastic finite element method;
- Green's function method;
- differential analysis methods.

The analytical methods need access to the governing model equations. These methods may include writing additional computer codes for the solution of the auxiliary equations. This may make analytical methods impractical and sometimes impossible. For instance, reformulating an existing computational model developed by others could require prohibitive amounts of resources.

Coupled/decoupled direct method

The coupled/decoupled direct method (CDDM) contains differentiation of the model equations and the subsequent solution of the sensitivity equations. In the coupled direct method, the sensitivity equations are then solved along with the original model equations (Tomović, 1972). In the decoupled direct method, the sensitivity equations and the original model equations are solved separately (Dunker, 1984; Prokopakis, 1993). The decoupled method has the advantage of computational efficiency and stability of the solution.

Spectral-based stochastic finite element method

The spectral-based stochastic finite element method relies on the use of representing stochastic processes in terms of a series expansion. This approach results in a set of linear matrix equations with deterministic matrices multiplied by random vectors for finite element method problems. The matrix equations are solved by using either the Galerkin's or method operator expansions (Villadsen, 1978).

Green's function method

The sensitivity equations of a model are obtained after differentiating the model equations. The sensitivity equations are solved with constructing an auxiliary set of Green's functions. This method reduces the number of differential equations solved for sensitivity, and replaces them with integrals that can be easily evaluated (Dougherty, 1979; Villadsen, 1978). Generally, The Green's function method is less efficient than the decoupled method (Tomović, 1972).

Differential analysis methods

The differential analysis methods use the Neumann expansion (Adomian, 1980; Dougherty, 1979a) and perturbation theory (Dougherty, 1979a; Tatang, 1992). Since the Neumann expansion method includes the inverse of the model, it may have some limitations. The perturbation methods include the expansion of the model outputs in terms of small random perturbations in model parameters.

Since application of these methods is complex for the non-linear systems and the perturbation terms must be small, the differential analysis methods have some limitations.

A1.4 Computer algebra-based methods

The computer algebra-based methods involve both the direct manipulation of the computer code and the estimation of the uncertainty and sensitivity of model outputs with respect to model inputs. These methods do not need information about the model structure or the model equations.

A1.5 UA/SA commonly used in the nuclear industry

Uncertainty methods for advanced best-estimate thermal-hydraulic code applications are addressed in a Nuclear Energy Agency report on uncertainty analysis methods (NEA, 1997). In this report, he provides detailed information on the uncertainty methods given below:

- AEA Technology method;
- University of Pisa method;
- GRS method;
- IPSN method;
- ENUSA method.

Appendix 2: PIRT information

Two independent expert groups worked at PSU on the Phenomena Identification Ranking Table (PIRT) tables (Tables A2.1 through A2.8) for void distribution (Aydogan, 2007a) and critical power (Aydogan, 2007) predictions. The steps of the development of the PIRT tables are given as:

- The first group developed the PIRT tables and ranked them. Three rankings were used: low, medium and high. The greater the effect on the uncertainty output parameter expected, the higher the ranking of the uncertainty parameter.
- The second group members reviewed the PIRT tables and provided their comments.
- Finally, the first group finalised the PIRT tables according to the second group's review.

The two expert groups agreed with each other for most of the parameters except for a few uncertain parameters ranks. Tables A2.9 and A2.10 demonstrate the disagreement and final decision about the PIRT tables for the cases of void distribution and critical power, respectively.

The BFBT benchmark participants may use the PIRT tables to obtain the most sensitive uncertain parameters or they can create their own uncertain parameters tables in order to use in their UA/SA. If they use PDF for the defined sensitive/uncertain parameters, they need to be presented to the benchmark team.

Table A2.1: PIRT-1 for steady-state void distribution

Boundary condition effect			
ID	Parameter	Ranking	Basis for ranking
1	Initial vessel operating pressure	M	This parameter affects the saturation temperature.
2	Flow rate in the bundle	H	This parameter is in the energy equation.
3	Power	H	This parameter is in the energy equation.
4	Inlet flow temperature	M	This parameter changes the inlet boundary condition.

L: Low, M: Medium, H: High.

Table A2.2: PIRT-2 for steady-state void distribution

Geometry effect			
ID	Parameter	Ranking	Basis for ranking
1	Wetted perimeter	L	This perimeter affects the friction factor.
2	Sub-channel area	H	This parameter affects the mass flow rate.
3	Nominal gap width	L	This parameter affects the lateral flow.
4	The distance between the centres of channels	L	This parameter affects the lateral flow.
5	Fraction of channel area blocked by grid	M	This parameter affects the pressure drop and the heat transfer. How effective this parameter affects the void distribution has to be shown with the sensitivity analysis.
6	Grid perimeter	M	How effectively this parameter affects the void distribution has to be shown with the sensitivity analysis.
7	Heated perimeter	H	This perimeter affects the heat flux and void distribution but the geometry of the bundle is well known.
8	Housing wetted perimeter	L	This perimeter affects the friction factor.

L: Low, M: Medium, H: High.

Table A2.3: PIRT-3 for steady-state void distribution

Model parameter effect – hydraulics			
ID	Parameter	Ranking	Basis for ranking
1	The loss coefficient for a gap – lateral	M	This parameter affects the lateral flow in bundle. The ranking of this parameter has to be determined with sensitivity analysis.
2	The wall friction factor for the gap	L	This affects the pressure drop.
3	The grid loss coefficient – axial	M	This parameter affects the pressure drop in the bundle. The ranking of this parameter has to be determined with sensitivity analysis.
4	The mixing coefficient	H	This parameter affects the lateral void distribution in the bundle
5	Equilibrium distribution weighing factor in void drift	H	This parameter affects the lateral void distribution in the bundle.
Interfacial mass transfer			
6	Interfacial friction factor	H	This parameter affects the pressure drop.
Interfacial drag force			
7	Drag coefficient for bubble flow regime	M	The ranking of this parameter has to be determined with sensitivity analysis.
8	Drag coefficient for drop flow regime	M	The ranking of this parameter has to be determined with sensitivity analysis.
9	Interfacial friction factor for film flow regime	H	This parameter affects the mass transfer between film flow and vapour.
Friction factor in wall drag force			
10	Single-phase friction factor in wall drag force	L	This affects the pressure drop.
11	Two-phase friction factor in wall drag force	M	This affects the pressure drop. Because two-phase pressure drop models have higher uncertainty, this parameter is ranked as M. The ranking of this parameter has to be determined with sensitivity analysis.

L: Low, M: Medium, H: High.

Table A2.4: PIRT-4 for steady-state void distribution

Model parameter effect – thermal			
ID	Parameter	Ranking	Basis for ranking
Wall heat transfer coefficient			
1	Single phase liquid	M	The ranking of this parameter has to be determined with sensitivity analysis.
2	Sub-cooled nucleate boiling	M	The ranking of this parameter has to be determined with sensitivity analysis.
3	Saturated boiling region	M	The ranking of this parameter has to be determined with sensitivity analysis.
Entrainment/deposition			
<i>Entrainment in film flow</i>			
4	Entrainment rate	M	The ranking of this parameter has to be determined with sensitivity analysis. This parameter has more importance in the post-CHF scenario.
<i>De-entrainment in film flow</i>			
5	De-entrainment rate for film flow	M	The ranking of this parameter has to be determined with sensitivity analysis.
<i>De-entrainment on grid spacers</i>			
6	S _{DE}	M	The ranking of this parameter has to be determined with sensitivity analysis.
<i>Spacer grid enhancement for entrained phase (to create thicker liquid film)</i>			
7	S _E	M	The ranking of this parameter has to be determined with sensitivity analysis.

L: Low, M: Medium, H: High.

Table A2.5: PIRT-1 for steady-state critical power

Boundary condition effect			
ID	Parameter	Ranking	Basis for ranking
1	Initial vessel operating pressure	M	This parameter affects the saturation temperature.
2	Flow rate in the bundle	H	This parameter is in the energy equation.
3	Power	H	This parameter is in the energy equation.
4	Inlet flow temperature	M	This parameter changes the inlet boundary condition.

L: Low, M: Medium, H: High.

Table A2.6: PIRT-2 for steady-state critical power

Geometry effect			
ID	Parameter	Ranking	Basis for ranking
1	Wetted perimeter	L	This perimeter affects the friction factor.
2	Sub-channel area	H	This parameter affects the mass flow rate.
3	Nominal gap width	L	This parameter affects the lateral flow.
4	The distance between the centres of channels	L	This parameter affects the lateral flow.
5	Fraction of channel area blocked by grid	M	This parameter affects the pressure drop and the heat transfer. How effectively this parameter affects the void distribution has to be shown with the sensitivity analysis.
6	Grid perimeter	M	How effectively this parameter affects the void distribution has to be shown with the sensitivity analysis.
7	Heated perimeter	H	This perimeter affects the heat flux and void distribution.
8	Housing wetted perimeter	L	This perimeter affects the friction.

L: Low, M: Medium, H: High.

Table A2.7: PIRT-3 for steady-state critical power

Model parameter effect – hydraulics			
ID	Parameter	Ranking	Basis for ranking
Wall heat transfer coefficient			
1	The loss coefficient for a gap – lateral-	L	This parameter affects the lateral flow in bundle. The ranking of this parameter has to be determined with sensitivity analysis.
2	The wall friction factor for the gap	L	This affects the pressure drop.
3	The grid loss coefficient – axial	M	This parameter affects the pressure drop in the bundle. The ranking of this parameter has to be determined with sensitivity analysis.
4	The mixing coefficient	H	This parameter affects the lateral void distribution in the bundle.
5	Equilibrium distribution weighing factor in void drift	H	This parameter affects the lateral void distribution in the bundle.
Interfacial mass transfer			
6	Interfacial friction factor	H	This parameter affects the pressure drop.
Interfacial drag force			
7	Drag coefficient for bubble flow regime	L	Drag coefficient affect the friction at the beginning of the bundle.
8	Drag coefficient for drop flow regime	M	The ranking of this parameter has to be determined with sensitivity analysis.
9	Interfacial friction factor for film flow regime	H	Because this parameter affects the drag force which is near the dry-out, it affects the dry-out.
Friction factor in wall drag force			
10	Single-phase friction factor in wall drag force	L	This affects the pressure drop.
11	Two-phase friction factor in wall drag force	M	This affects the pressure drop. Because two-phase pressure drop models have higher uncertainty, this parameter is ranked as M. The ranking of this parameter has to be determined with sensitivity analysis.

L: Low, M: Medium, H: High.

Table A2.8: PIRT-4 for steady-state critical power

Model parameter effect – thermal			
ID	Parameter	Ranking	Basis for ranking
Wall heat transfer coefficient			
1	Single phase liquid	M	The ranking of this parameter has to be determined with sensitivity analysis.
2	Sub-cooled nucleate boiling	M	The ranking of this parameter has to be determined with sensitivity analysis.
3	Saturated boiling region	M	The ranking of this parameter has to be determined with sensitivity analysis.
Entrainment/deposition			
<i>Entrainment in film flow</i>			
4	Entrainment rate	H	Entrainment affects the liquid film rate.
<i>De-entrainment in film flow</i>			
5	De-entrainment rate for film flow	H	De-entrainment affects the liquid film rate.

L: Low, M: Medium, H: High.

Table A2.9: Comparison of two independent expert groups' decisions about the PIRT tables for the void distribution

Effect	Parameter(s)	First group's decision	Second group's decision
Boundary condition effect	Inlet temperature	L	M (If the inlet temperature is increased, the exit temperature of the coolant will change for a fixed power.)
Geometry effect	All	Agreement	Agreement
Hydraulic effect	The loss coefficient for a gap	L	M (If the lateral cross loss coefficient is increased, there will be no cross-flow. Void drift and mixing coefficient may not be effective in that case.)
Hydraulic effect	Interfacial friction factor in mass transfer and interfacial drag force	H	H (Although interfacial drag coefficient is used by two equations, its effect may be different on the result. Therefore, the ranking of this parameter may be different in each equation. The group suggests changing the ranking of the interfacial friction factor in interfacial drag force eq. to Medium.)
Thermal effect	All	Agreement	Agreement

Table A2.10: Comparison of two independent expert groups' decisions about the PIRT tables for the critical power

Effect	Parameter(s)	First group's decision	Second group's decision
Boundary condition effect	Inlet temperature	L	M (If the inlet temperature is increased, the exit temperature of the coolant will change for a fixed power.)
Geometry effect	All	Agreement	Agreement
Hydraulic effect	All	Agreement	Agreement
Hydraulic effect	Interfacial friction factor in mass transfer and interfacial drag force	H	H (Although interfacial drag coefficient is used by two equations, its effect may be different on the result. Therefore, the ranking of this parameter may be different in each equation. The group suggests changing the ranking of the interfacial friction factor in interfacial mass transfer eq. to Medium.)
Hydraulic effect	Drag coefficient for bubble flow regime	L	M (Suggested that sensitivity analyses are needed to understand its effect.)
Thermal effect	All	Agreement	Agreement

OECD PUBLICATIONS, 2 rue André-Pascal, 75775 PARIS CEDEX 16
Printed in France.